Supporting Information

Multiple Heteroatom-Doped Few-Layer Carbons for Electrochemical Oxygen Reduction Reaction

Baobing Huang,[a] Yuchuan Liu,[a] Xing Huang[b,c] and Zailai Xie*[a]*

[a]*State Key Laboratory of Photocatalysis on Energy and Environment, College of Chemistry, Fuzhou University, Fuzhou 350116, P. R. China*

Email: zlxie@fzu.edu.cn

[b]*Department of Inorganic Chemistry, Fritz Haber Institute of Max Planck Society, Faradayweg 4-6, 14195 Berlin, Germany*

Email: xinghuang@fhi-berlin.mpg.de, xinghuang0214@mail.ipc.ac.cn

[c]*Department of Heterogeneous Reations, Max Planck Institute for Chemical Energy Conversion, 45470, Mülheim an der Ruhr, Germany*

Figures and captions

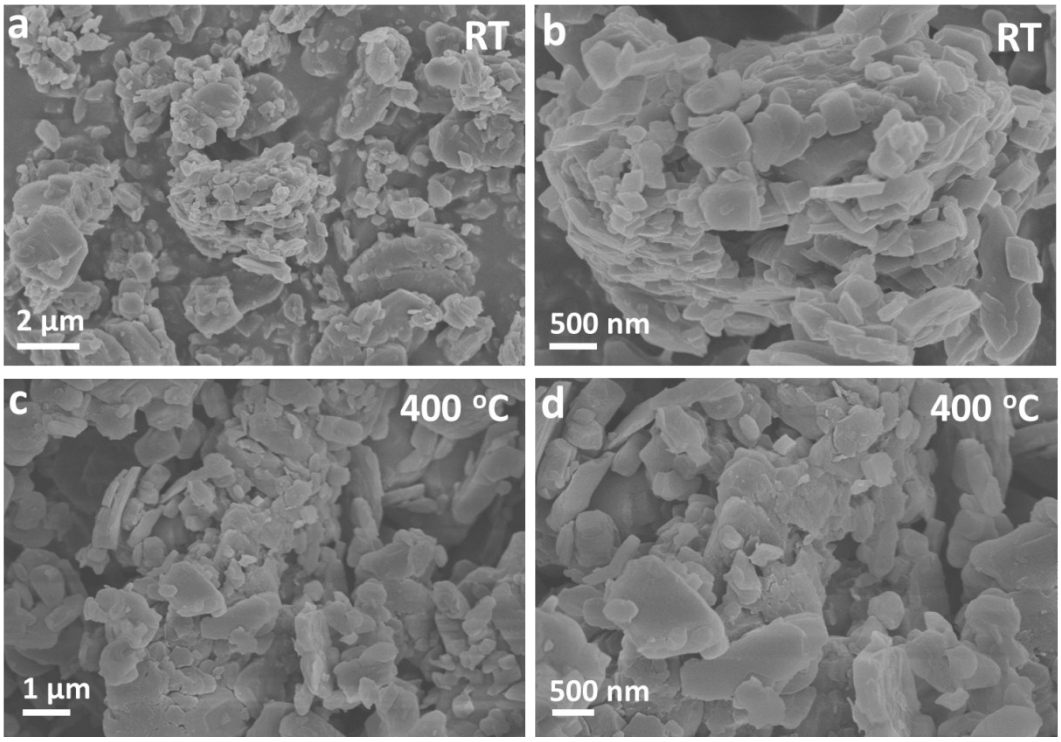

Figure S1. SEM images of aggregates of guanine recorded at RT and after annealing at 400 °C for 1h in N_2. Comparing to the morphology of initial state, no detectable changes are observed after heating at 400 °C.

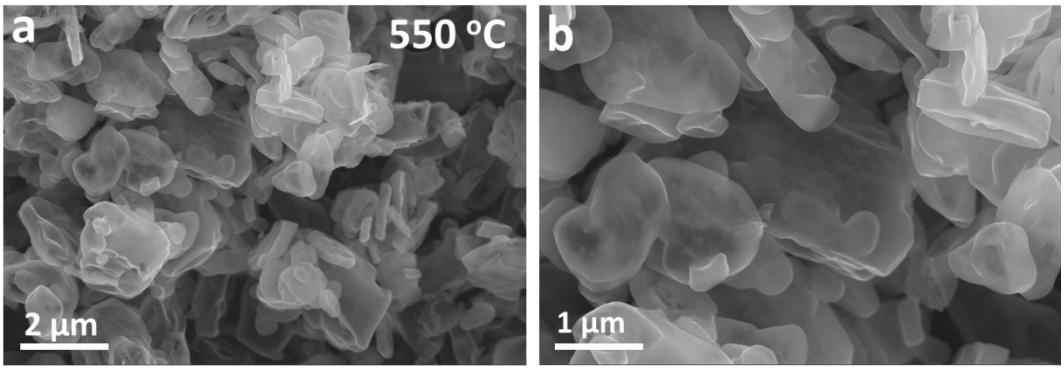

Figure S2. SEM images of aggregates of guanine recorded after annealing at 550 °C for 1 h in N_2. One can already see that the morphology starts to change: a slight depression or indentation in surfaces of particles occurs. The amount of small particles is decreased, which could be due to the incorporation of them into bigger ones.

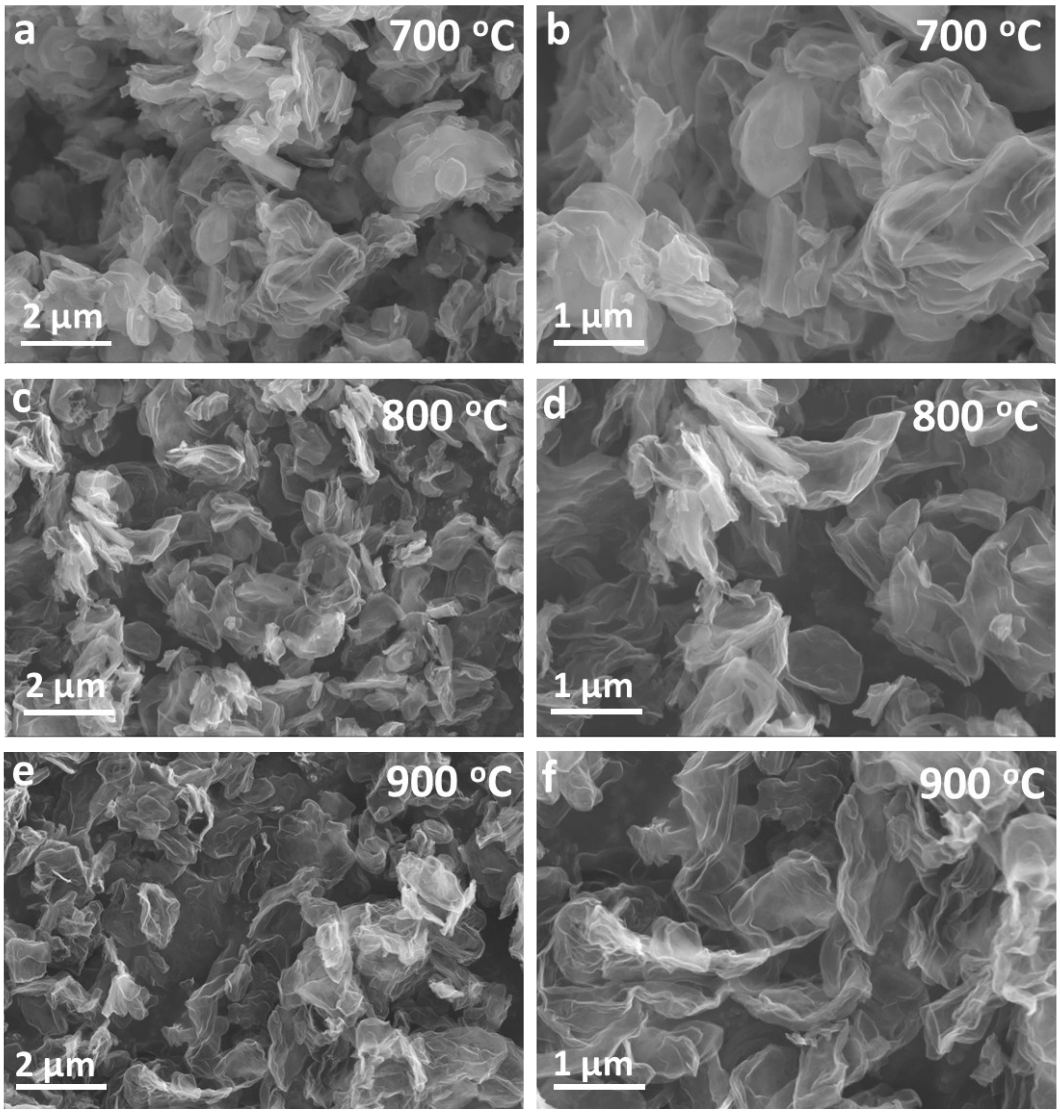

Figure S3. SEM images of aggregates of guanine recorded after annealing at (a) 700 °C, (b) 800 °C and (c) 900 °C for 1 h in N_2. One can observe that at 700 °C, most of particles have been transformed into 2D nanosheets. The sheets become thinner and more crumped at increased temperature (800-900°C).

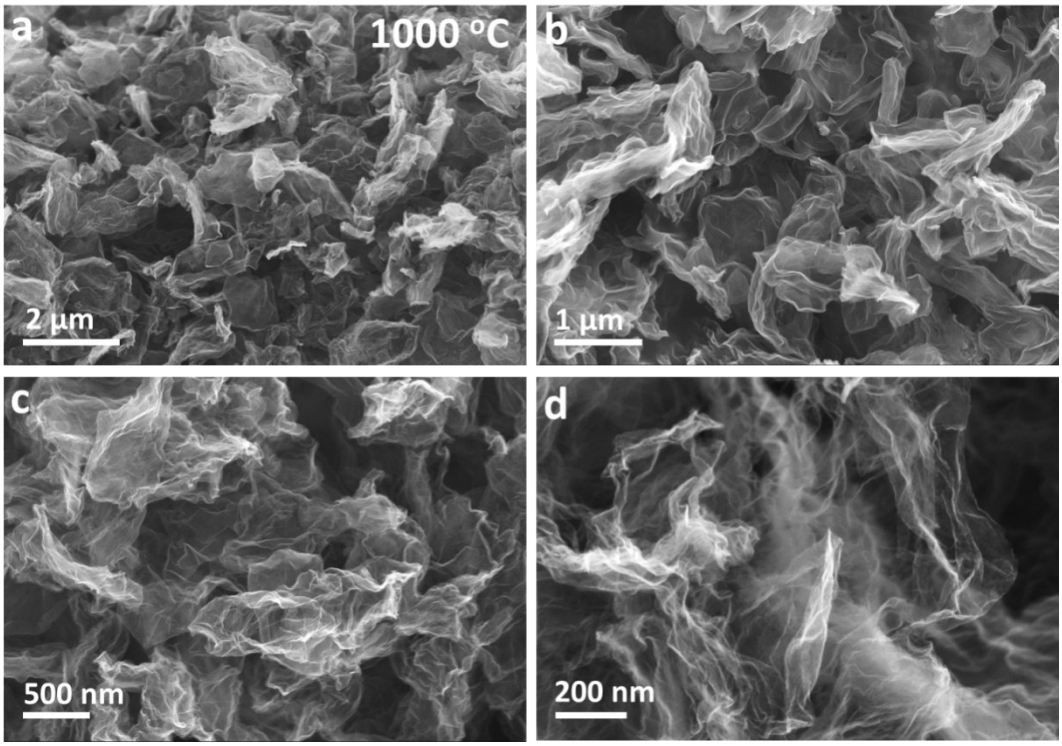

Figure S4. SEM images of aggregates of guanine recorded at 1000 °C for 1 h in N_2, showing the formation of 2D carbon nanosheets.

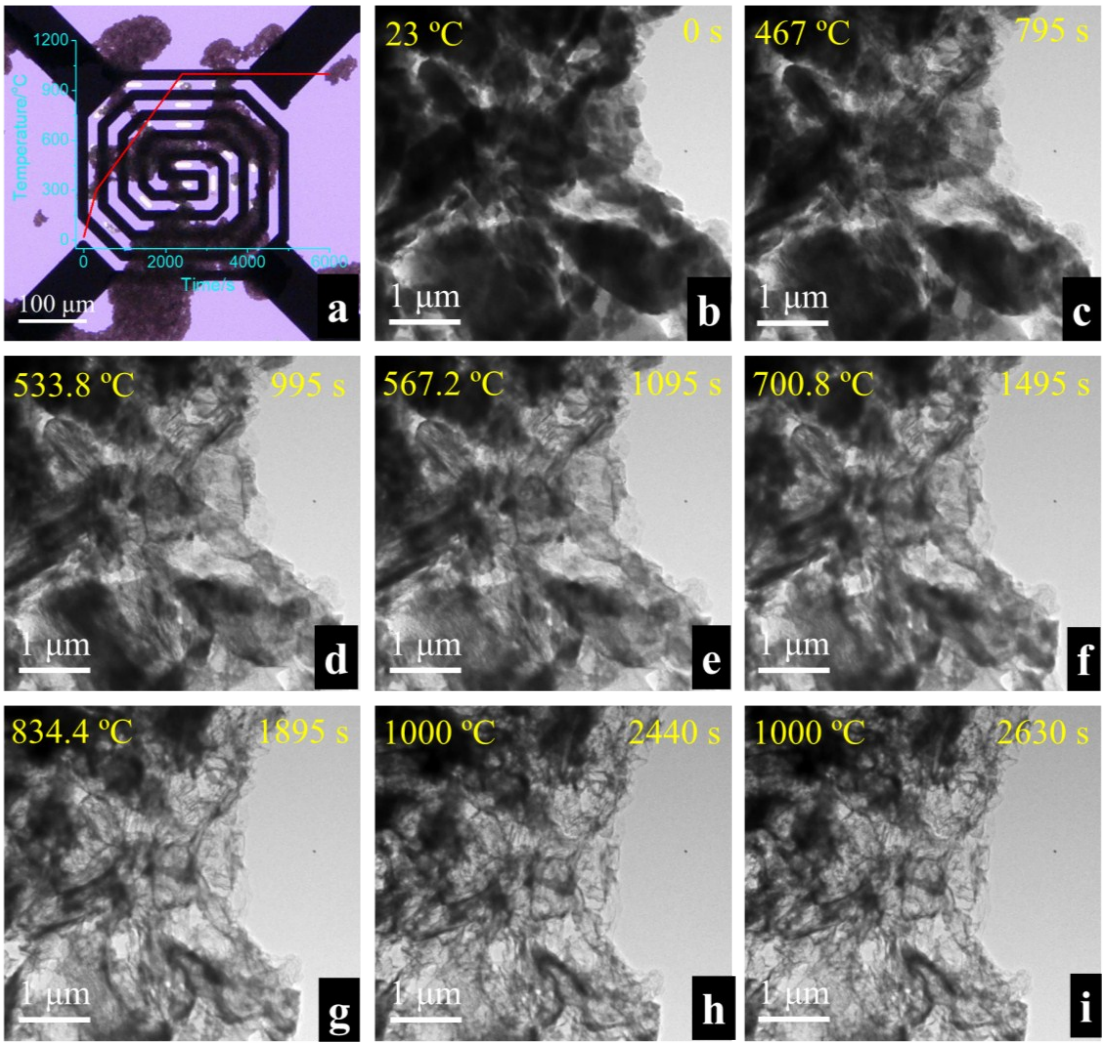

Figure S5. (a) An optical photograph of MEMS-based heating chip for *in situ* heating experiment; inset shows the temperature profile. (b-i) A series of time-resolved TEM images recorded during *in situ* heating experiment, showing morphological transformation of precursor material from 3D aggregated particles to large size 2D sheet-like structures.

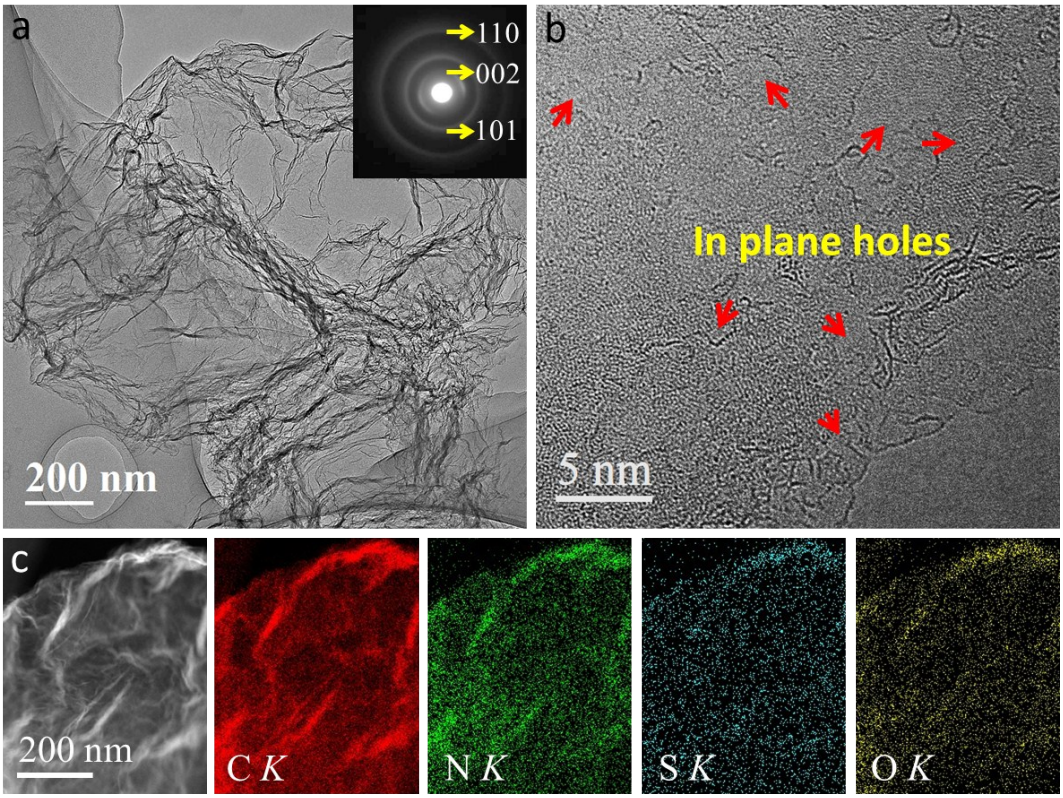

Figure S6. (a) TEM and (b) HRTEM images of the GS-1000; Inset of (a) shows the SAED pattern; (c) HAADF-STEM image and corresponding elemental maps of C, N, S and O, respectively. The ultrathin and defective nature of the nanosheets can be clearly revealed by TEM characterization. The elemental mapping analysis shows that the doping elements, i.e., N, S, and O, are homogeneously distributed over the carbon nanosheet.

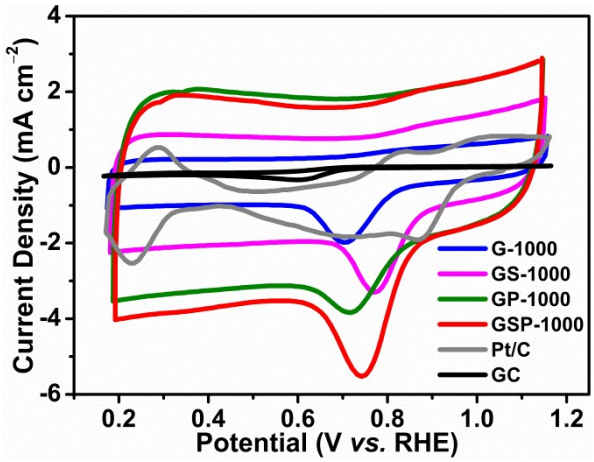

Figure S7. CVs of different samples in O_2-saturated 0.1 M KOH solution with 50 mV s^{-1}.

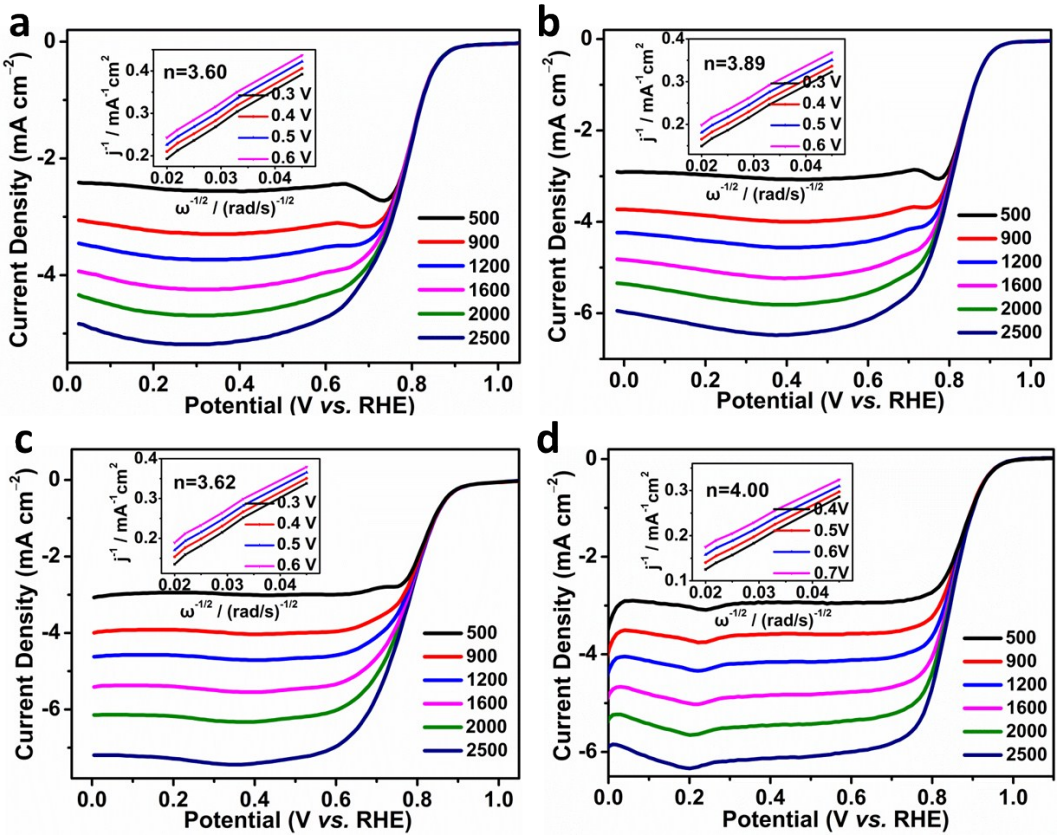

Figure S8. LSV curves of (a) G-1000, (b) GS-1000, (c) GP-1000 and (d) Pt/C at different rpms in O_2-saturated 0.1 M KOH solution.

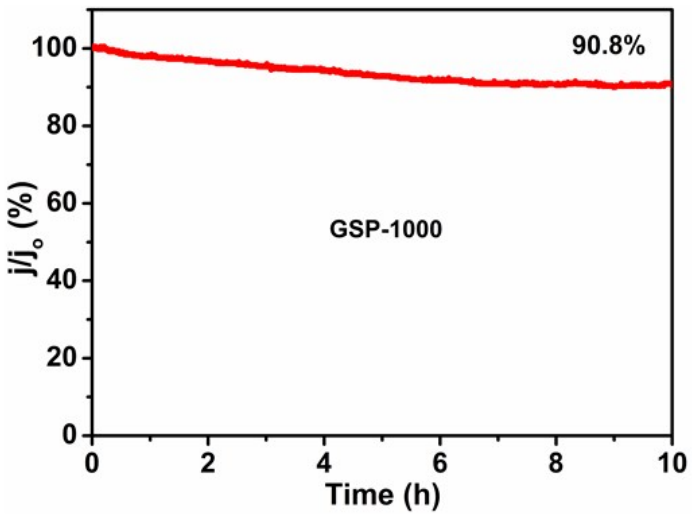

Figure S9. Current-time response at 0.8 V (vs. RHE) in O_2-saturated 0.1 M KOH solution at a rotation rate of 1600 rpm.

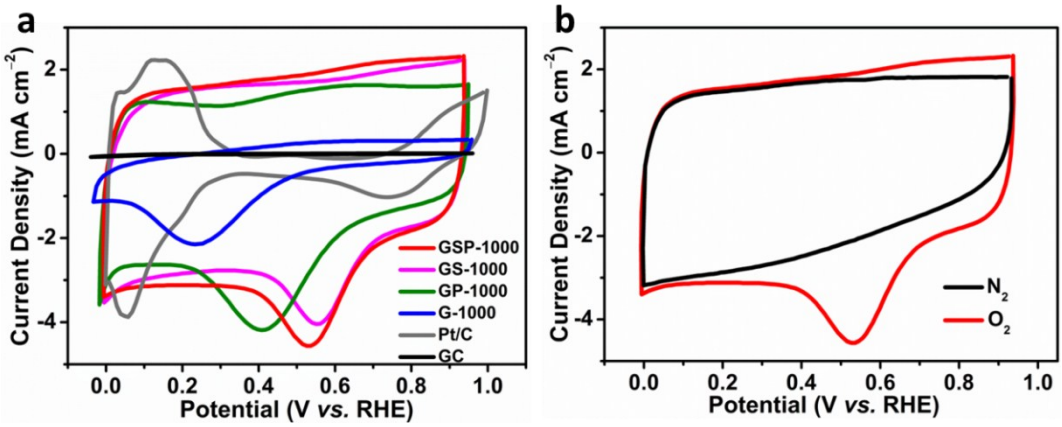

Figure S10. (a) CVs in O_2-saturated 0.1 M $HClO_4$ solution with 50 mV s^{-1}. (b) CVs of GSP-1000 in N_2 or O_2-saturated 0.1 M $HClO_4$ solution.

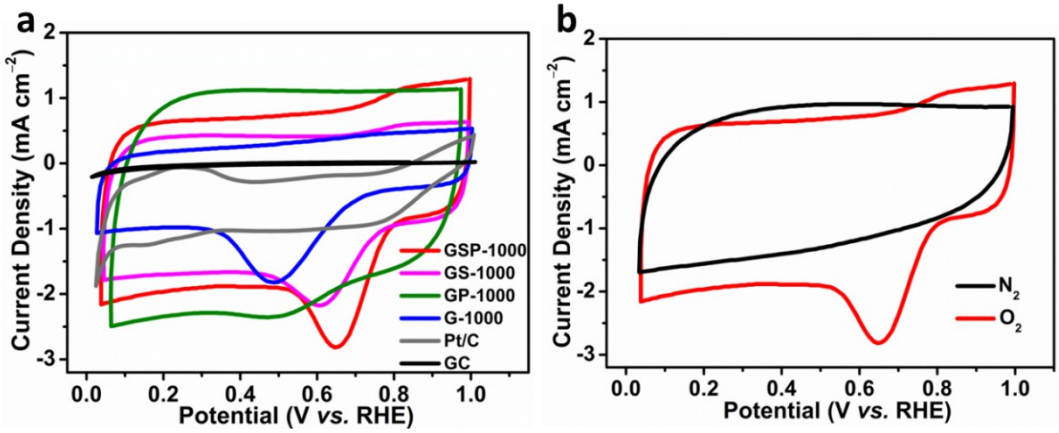

Figure S11. (a) CVs in O_2-saturated 0.1 M PBS with 50 mV s^{-1}. (b) CVs of GSP-1000 in N_2 or O_2-saturated 0.1 M PBS.

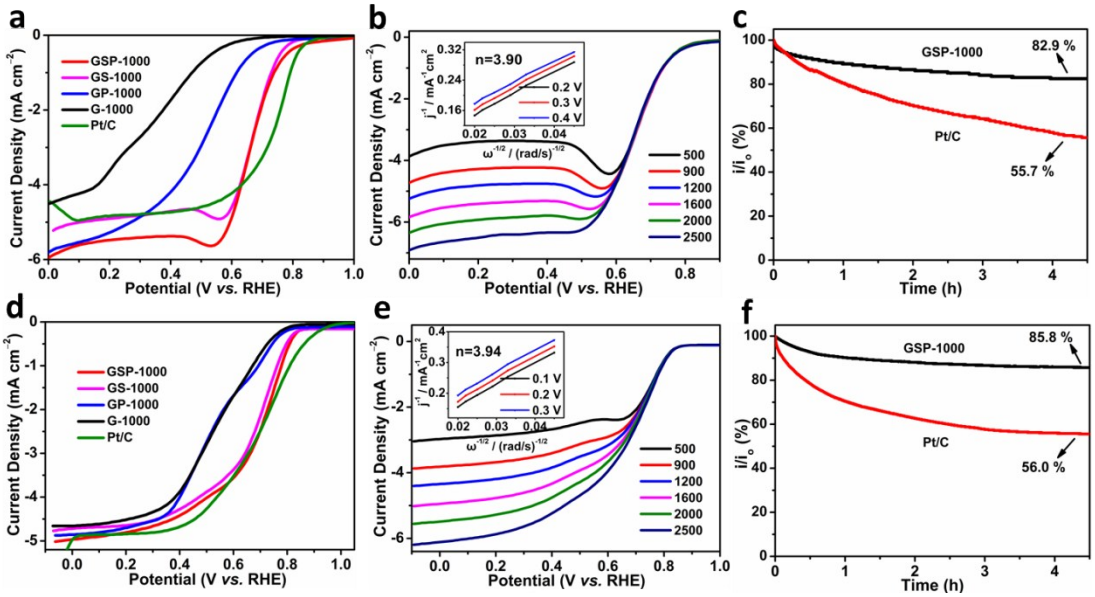

Figure S12. (a-c) In O_2-saturated 0.1 M $HClO_4$ solution: (a) LSV curves at 1600 rpm with 10 mV s^{-1}, (b) LSV curves of GSP-1000 at different rpms, (c) i–t response at 0.65 V (*vs.* RHE) at 1600 rpm. (d-f) In O_2-saturated 0.1 M PBS: (d) LSV curves at 1600 rpm with 10 mV s^{-1}, (e) LSV curves of GSP-1000 at different rpms, (f) i–t response at 0.65 V (*vs.* RHE) at 1600 rpm.

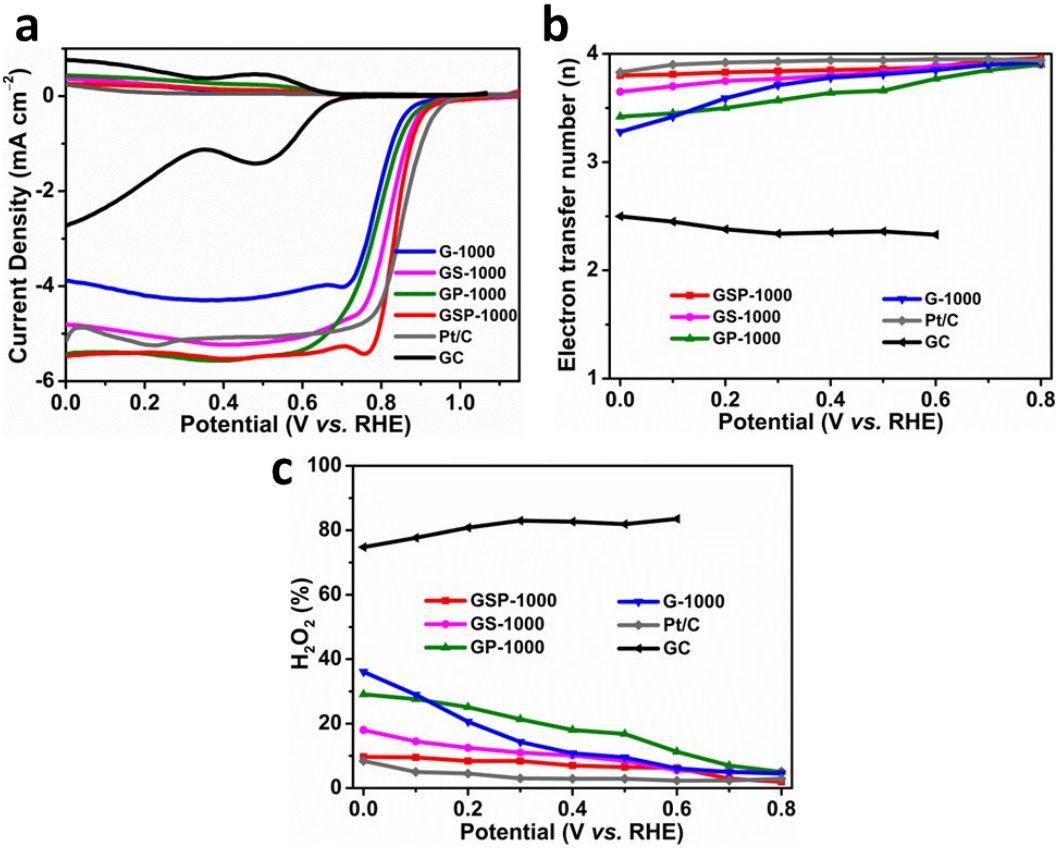

Figure S13. (a) RRDE voltammograms, (b) corresponding electron transfer numbers and (c) peroxide percentage of different samples at 1600 rpm in O_2-saturated 0.1 M KOH.

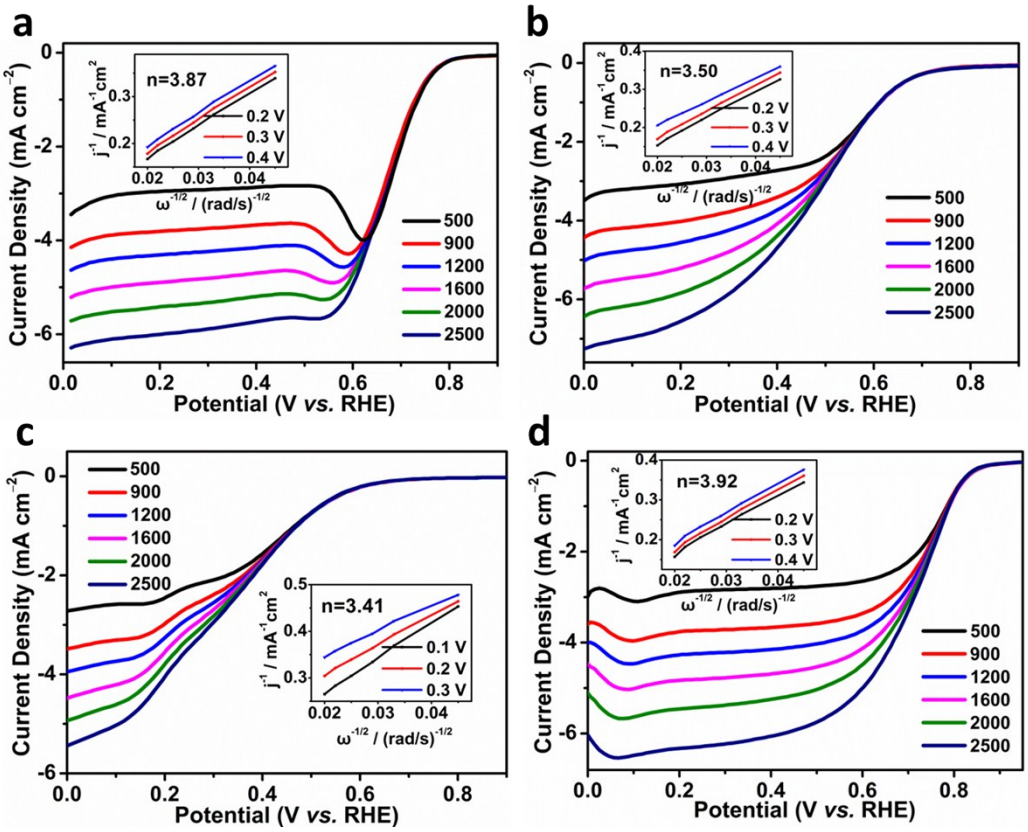

Figure S14. (a), (b), (c) and (d) LSV curves at different rpms for GS-1000, GP-1000, G-1000 and Pt/C, respectively, in O_2-saturated 0.1 M $HClO_4$ solution.

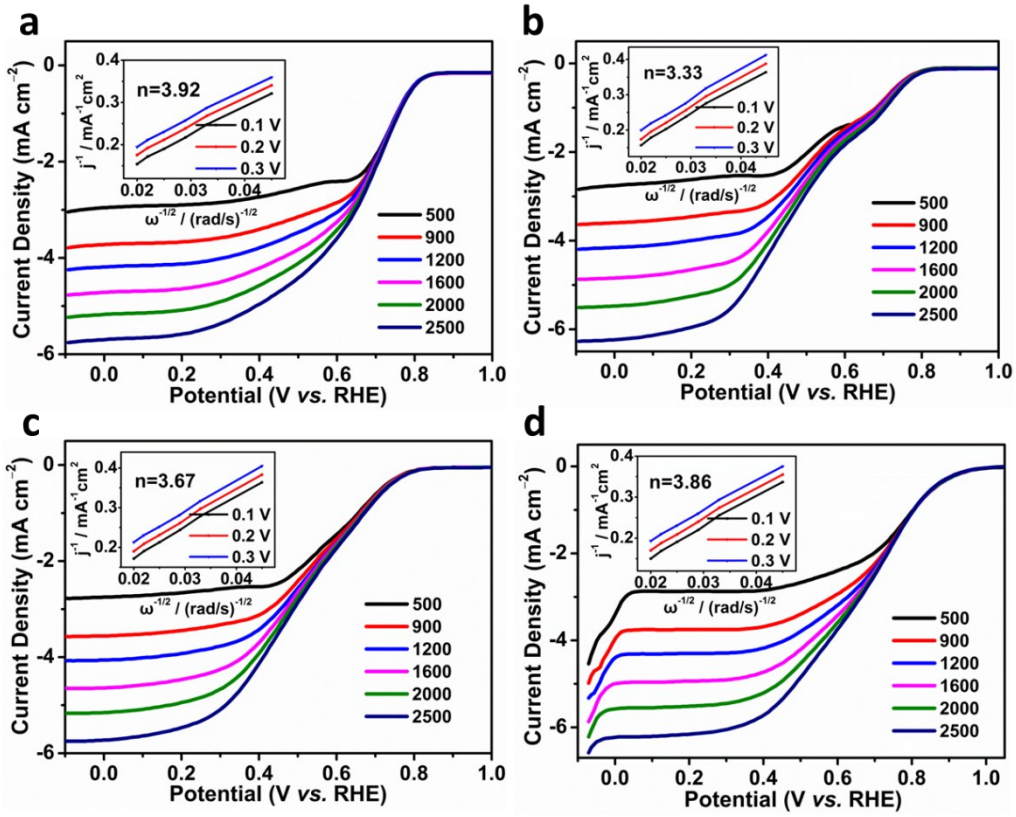

Figure S15. (a), (b), (c) and (d) LSV curves at different rpms for GS-1000, GP-1000, G-1000 and Pt/C, respectively, in O_2-saturated 0.1 M PBS.

Discussion: As displayed in Figure S10 and Figure S11, both GSP-1000 and GS-1000 keep significant oxygen reduction characteristic peaks in O_2-saturated 0.1 M $HClO_4$ and 0.1 M PBS (phosphate buffer solution, pH = 7.0). The LSV curves in Figure S12a and d further confirm that both GSP-1000 and GS-1000 possess comparable onset and half-wave potentials to those of Pt/C catalyst. In acid electrolyte, GSP-1000 even shows larger diffusion-limited current density. The average electron transfer numbers calculated from K-L plots both are up to 3.9, indicative of a favorable 4e transferring pathway (Figure S12b and e). Moreover, the current retention rates of GSP-1000 maintain at 83% in acid medium and 86% in neutral medium, notably outperforming those of Pt/C catalyst (both around 56%) after more than 4 h stability-testing (Figure S12c and f). All above results demonstrate the outstanding ORR performances of our 2D carbons based unique electrocatalysts in universal pH conditions, which outperforms most of graphene-based electrocatalysts and even some advanced Fe-based ORR catalysts (Table S2-S3).

Table S1. ORR performances of the samples presented in the article.

	0.1 M KOH			0.1 M $HClO_4$			0.1 M PBS		
Catalysts	E_{onset} (V *vs.* RHE)	$E_{1/2}$ (V *vs.* RHE)	$\|j_L\|$ (mA cm^{-2})	E_{onset} (V *vs.* RHE)	$E_{1/2}$ (V *vs.* RHE)	$\|j_L\|$ (mA cm^{-2})	E_{onset} (V *vs.* RHE)	$E_{1/2}$ (V *vs.* RHE)	$\|j_L\|$ (mA cm^{-2})
GSP-1000	0.99	0.84	5.40	0.89	0.67	5.48	0.90	0.70	4.83
GS-1000	0.98	0.82	5.10	0.88	0.68	4.91	0.89	0.69	4.67
GP-1000	0.95	0.79	5.40	0.82	0.52	5.27	0.85	0.53	4.70
G-1000	0.95	0.79	4.21	0.79	0.39	3.67	0.87	0.54	4.51
Pt/C	1.03	0.85	5.10	0.95	0.74	4.84	1.02	0.71	4.84

j_L is determined at 0.2 V (*vs.* RHE).

Table S2. Comparison of some advanced graphene-based ORR catalysts in 0.1 M KOH electrolyte.

Catalysts	Synthetic method	E_{onset} (V *vs.* RHE)	$E_{1/2}$ (V *vs.* RHE)	$\|j_L\|$ @1600 rpm (mA cm^{-2})	References
B, N-doped graphene	Two-step pyrolysis (GO, NH_3, H_3BO_3)	0.86	0.68	5.2	*Angew. Chem. Int. Ed.* 2013, 52, 3110
N, S-doped graphene	Pyrolysis (GO, 2-aminothiophenol)	0.87	0.61	1.8	*Adv. Mater.* 2014, 26, 6186
N, P, S -doped graphene	Pyrolysis (GO, triphenylphosphine, and thiourea)	-0.03 V (vs. Ag/AgCl)	-	6.4	*Carbon* 2014, 78, 257
N, S-doped carbon nanosheets	Pyrolysis (GO, dopamine and 2-mercaptoethanol)	0.92	0.77	4.3	*Nano Energy* 2016, 19, 373
N, P, F-doped graphene	Pyrolysis (polyaniline, GO, and NH_4PF_6)	0.90	0.71	6.0	*Angew. Chem. Int. Ed.* 2016,55, 13296
Defect graphene	Annealing at 1150 °C (N-doped G)	0.91	0.76	4.5	*Adv. Mater.* 2016, 28, 9532
Defect graphene	Ar plasma etching (GO)	0.91	0.74	-	*Chem. Commun.* 2016, 52, 2764
N, P-doped CNT/graphene hybrid nanospheres	Multiple-step treatment and annealing	0.94	0.82	5.6	*Adv. Mater.* 2016, 28, 4606
N/S/P/O-doped GSP-1000	**Annealing (GSP)**	**0.99**	**0.84**	**5.4**	**This work**
N/S/O-doped GS-1000	**Annealing (GS)**	**0.98**	**0.82**	**5.1**	**This work**
N/P/O-doped GP-1000	**Annealing (GP)**	**0.95**	**0.79**	**5.4**	**This work**

Table S3. Comparison of some advanced ORR catalysts in acidic electrolyte.

Catalysts	E_{onset} (V *vs.* RHE)	$E_{1/2}$ (V *vs.* RHE)	$\|j_L\|$ @1600 rpm (mA cm^{-2})	Electrolyte	References
N-doped mesoporous carbon	0.8	0.5	4.5	0.1 M $HClO_4$	*J. Am. Chem. Soc.* 2011, 133, 206
N-doped spheres	0.65	0.42	5.5	0.5 M H_2SO_4	*Adv. Mater.* 2013, 25, 998
N-doped meso/micro porous carbon	0.84	0.72	4.6	0.5 M H_2SO_4	*Nature Commun.* 2014, 5, 4973
N -doped mesoporous carbon sheet	0.75	0.57	5.0	0.5 M H_2SO_4	*Angew. Chem. Int. Ed.* 2014, 53, 1570
N, P-doped mesoporous carbon	0.82	0.62	5.6	0.1 M $HClO_4$	*Nature Nanotech.* 2015, 10, 444
N, P-doped CNT/graphene hybrid nanospheres	0.9	0.68	5.7	0.1 M $HClO_4$	*Adv. Mater.* 2016, 28, 4606
Fe-N-C	0.82	0.60	6.0	0.1 M $HClO_4$	*J. Am. Chem. Soc.* 2014, 136, 11027
Fe_3C-C	0.9	0.73	5.5	0.1 M $HClO_4$	*Angew. Chem. Int. Ed.* 2014, 53, 3675
Fe_3C-CNT	0.89	0.63	6.0	0.5 M H_2SO_4	*J. Am. Chem. Soc.* 2015, 137, 1436
Fe-N-C nanofiber	0.84	0.62	5.0	0.5 M H_2SO_4	*Angew. Chem. Int. Ed.* 2015, 54, 8179
Fe-N doped carbon capsules	0.80	0.52	3.5	0.5 M H_2SO_4	*ACS Nano* 2016, 10, 5922
N/S/O-doped GS-1000	**0.88**	**0.68**	**4.9**	**0.1 M $HClO_4$**	**This work**
N/S/P/O-doped GSP-1000	**0.89**	**0.67**	**5.5**	**0.1 M $HClO_4$**	**This work**